Air Toxics Hot Spots Program

p-Chloro-*α,α,α*-trifluorotoluene
(*p*-Chlorobenzotrifluoride, PCBTF)

Cancer Inhalation Unit Risk Factor
Technical Support Document for
Cancer Potency Factors
Appendix B

August 2020

Air and Site Assessment and Climate Indicator Branch
Office of Environmental Health Hazard Assessment
California Environmental Protection Agency

Page Intentionally Left Blank

p-Chloro-*α,α,α*-trifluorotoluene (*p*-Chlorobenzotrifluoride, PCBTF) Cancer Inhalation Unit Risk Factor

Technical Support Document for Cancer Potency Factors

Appendix B

Office of Environmental Health Hazard Assessment (OEHHA)

Lauren Zeise, Ph.D., Director

Prepared by
Ken Kloc, Ph.D., MPH
Nygerma L. Dangleben, Ph.D.
John D. Budroe, Ph.D.

Technical Reviewers
David Siegel, Ph.D.
John D. Budroe, Ph.D.

August 2020

TABLE OF CONTENTS

LIST OF ACRONYMS	
AIC	Akaike information criterion
AUC	Area under the concentration curve
BMD	Benchmark dose
BMDL	Benchmark Dose Lower Bound
BMDS	Benchmark dose software
BMR	Benchmark Response
BW	Body weight
CSF	Cancer slope factor
CYP450	Cytochrome P450
DNA	Deoxyribose nucleic acid
Glu	Glucuronate
GSH	Glutathione
GST	Glutathione-S-transferase
HEC	Human equivalent concentration
IARC	International Agency for Research on Cancer
IR	Inhalation rate
IRIS	Integrated risk information system
IUR	Inhalation unit risk
kg	Kilogram
Km	Michaelis constant
LADD	Lifetime average daily dose
m^3/day	Cubic meters per day
mg/kg-day	Milligram per kilogram per day
mg/m^3	Milligram per cubic meter
$\mu g/m^3$	Microgram per cubic meter
NCI	National Cancer Institute
NRC	National Research Council
NTP	National Toxicology Program
PBPK	Physiologically-based pharmacokinetic
PCBTF	Parachlorobenzotrifluoride
ppb	Parts per billion
ppm	Parts per million
SCE	Sister chromatid exchange
TAC	Toxic air contaminant
TSD	Technical support document
UDS	Unscheduled DNA synthesis
US EPA	US Environmental Protection Agency
Vmax	Maximum velocity in Michaelis-Menton equation

INTRODUCTION

This document summarizes the carcinogenicity and derivation of cancer inhalation unit risk factors (IURs) for *p*-chloro-*α,α,α*-trifluorotoluene, also known and referred to hereinafter, as *p*-chlorobenzotrifluoride (PCBTF). Cancer unit risk factors are used to estimate lifetime cancer risks associated with inhalation exposure to a carcinogen.

The Office of Environmental Health Hazard Assessment (OEHHA) is required to publish guidelines for conducting health risk assessments under the Air Toxics Hot Spots (Hot Spots) program (Health and Safety Code Section 44360(b)(2)). In implementing this requirement, OEHHA develops cancer IURs for carcinogenic air pollutants.

In April 2018, the South Coast Air Quality Management District (SCAQMD) requested that OEHHA evaluate the carcinogenicity of PCBTF and if appropriate, develop an IUR for use in Hot Spots facility health risk assessments and other Air District activities. SCAQMD currently exempts PCBTF from VOC emission control regulations under SCAQMD Rule 102.

The IUR for PCBTF was developed using the methodology described in OEHHA's "Air Toxics Hot Spots Program Technical Support Document for Cancer Potency Factors" (OEHHA, 2009).

Major Sources and Uses

PCBTF is used in the preparation of dyes, pharmaceuticals, pesticides, and as a solvent in paints, inks, and high-solids coating formulations, as well as for metal cleaning. The US Environmental Protection Agency's (US EPA) Chemical Data Report database, developed under the Toxic Substances Control Act, indicates that total production and import of PCBTF in the US was 5,000 to 25,000 tons per year from 2012 through 2015 (US EPA, 2016). Five businesses in California submitted "quantity used" information to this database, but this information was not available to OEHHA because it is classified as confidential business information.

Air Emissions and Exposure Potential

OEHHA did not locate any data or other information on air emissions of, or exposures to, PCBTF in California.

However, in an air pollution study of secondary organic aerosol formation (Shah et al., 2019), ambient PCBTF air concentrations were measured immediately downwind of painting activities at two Pittsburgh, Pennsylvania construction sites. PCBTF levels measured over several minutes were mostly low (< 1 μg/m^3) but displayed several peaks between 4 and 8 μg/m^3.

OEHHA did not locate any other non-occupational exposure data for California or other states except for a 1979 report of fish sampled from the Niagara River that were found to contain 0.17 – 2.0 parts per million (ppm) of PCBTF (Yurawecz, 1979).

Exposure to PCBTF could possibly occur from the use of products that contain PCBTF, or from contact with groundwater or soil contaminated with the chemical. In addition, PCBTF exposure may arise from consumption of some food products.

Exposure can also occur at workplaces where PCBTF is produced or used. In one recent study of occupational exposure at several US vehicle and paint manufacturing plants, workers were exposed to air concentrations of up to 12.2 ppm (90 mg/m^3), as a time-weighted average (Lee, et al., 2015).

Non-Cancer Effects

The primary purpose of this document is to evaluate the carcinogenicity of PCBTF and develop cancer potency factors for inhalation exposure to this chemical. Nonetheless, it is useful to briefly review the adverse non-cancer effects that may be caused by multiple exposures to PCBTF.

Human Studies

No studies on the non-cancer toxicity of PCBTF to humans were found in the peer-reviewed literature.

Animal Studies

OEHHA identified four peer-reviewed reports evaluating the sub-chronic or chronic, non-cancer effects of PCBFT exposure in rats and mice:

- A report of 14-week and two-year inhalation studies in rats and mice that evaluated both non-cancer and cancer effects (NTP, 2018).

- A paper on four- and 14-week inhalation studies in rats (Newton et al., 1998).

- A report of two-week, oral gavage studies in rats and mice (NTP, 1992).

- A paper on a four-week oral gavage study in rats (Macri *et al.*, 1987).

Exposure concentrations ranged from 10 to 2000 ppm (74 to 15,000 mg/m^3) in the inhalation studies, and from 10 to 1000 milligrams per kilogram of bodyweight per day (mg/kg-day) in the oral studies. The tables provided at the end of this introduction provide a detailed listing of the adverse and potentially adverse effects seen in these studies. Focusing more briefly on the inhalation studies by NTP (2018) and Newton et al. (1998), effects observed in rats and/or mice at the lower exposure levels (100 to 300 ppm; 740 to 2200 mg/m^3) included:

- Lung: pulmonary inflammation, fibrosis, hemorrhage, and epithelial hyperplasia

- Liver: Increased weight, hepatocyte hypertrophy, fatty changes, altered blood chemistry indicative of liver damage, eosinophilic focus

- Kidney: Increased weight, increased protein droplet formation, eosinophilic granules, and increased nephropathy (male rat)

- Decreased sperm motility and altered estrous cycle

- Harderian gland degeneration[1]

- Hyperplasia of the adrenal medulla and forestomach

- Increased endometrial atypical hyperplasia

At the higher exposure levels (400 to 2000 ppm; 3000 to 15,000 mg/m^3), additional effects were observed such as: hepatocellular necrosis, adrenal cortex vacuolation, decreased thymus weight, squamous epithelial hyperplasia of the larynx, nasal exudate, hyperactivity and tremor, and decreased cauda and epididymal weight.

---

[1] The Harderian gland is an exocrine gland that is located in the posterior ocular orbital of rodents and occurs in other tetrapods that possess a nictitating membrane. Its functions include lubrication of the conjunctiva and the production of pheromones.

Non-Neoplastic Effects of Exposure to PCBTF in Mice and Rats[2]

NTP, 2018: Rat, Subchronic, Inhalation, 14 wk, 6 hr/d, 5 d/wk Tests Completed: Hematology and clinical chemistry, macro and microscopic pathology		
Exposure Levels		**Treatment-Related Effects**
ppm	**mg/m^3**	
2000	15,000	-Adrenal cortex vacuolation -Decreased cauda and epididymal weight (m) -Altered estrous cycle (f)
1000	7400	-Centrilobular hepatocellular hypertrophy -Mammary gland hyperplasia (f) -Decreased sperm motility and number (m)
500	3700	-Increased liver weight (f) -Altered blood chemistry
250	1800	-Increased liver weight (m) -Centrilobular hepatocellular hypertrophy (m) -Increased kidney weight (m) -Harderian gland degeneration
125	920	-No observed effects

---

[2] Effects in males and females are designated as (m) and (f), respectively.

NTP, 2018: Mouse, Subchronic, Inhalation, 14 wk, 6 hr/d, 5 d/wk Tests Completed: Macro and microscopic pathology		
Exposure Levels		**Treatment-Related Effects**
ppm	**mg/m³**	
2000	15,000	-Decreased thymus weight -Adrenal cortex hypertrophy, X-zone degeneration (f) -Forestomach granulomatous inflammation
1000	7400	-Hepatocellular necrosis, multinucleated hepatocytes (f) -Hematopoietic cell proliferation in the spleen (m)
500	3700	-Centrilobular hepatocellular hypertrophy (f) -Hepatocellular necrosis, multinucleated hepatocytes (m) -Increased kidney weight (m) -Forestomach epithelial hyperplasia
250	1800	-Increased liver weight -Centrilobular hepatocellular hypertrophy (m) -Hematopoietic cell proliferation in the spleen (f)
125	920	-Decreased sperm motility (m) -Altered estrous cycle (f)

NTP, 2018: Rat, Chronic, Inhalation, 2 yr, 6 hr/d, 5 d/wk Tests Completed: Macro and microscopic pathology		
Exposure Levels		**Treatment-Related Effects**
ppm	**mg/m³**	
1000	7400	-Pulmonary hemorrhage (f) -Liver foci: eosinophilic (m), mixed cell (f), and clear cell (f) -Nasal exudate (m)
300	2200	-Pulmonary fibrosis (f) -Centrilobular hepatocellular hypertrophy (f) -Fatty changes in liver -Adrenal medulla hyperplasia (f)
100	740	-Chronic lung inflammation -Pulmonary fibrosis (m) and hemorrhage (m) -Centrilobular hepatocellular hypertrophy (m) -Dose-dependent increase in severity of nephropathy (m) -Dose-dependent increase in endometrial atypical hyperplasia (f)

NTP, 2018: Mouse, Chronic, Inhalation, 2 yr, 6 hr/d, 5 d/wk Tests Completed: Macro and microscopic pathology		
Exposure Levels		**Treatment-Related Effects**
ppm	**mg/m³**	
400	3000	-Hepatocyte necrosis -Multinucleated hepatocytes (f) -Liver eosinophilic focus (m) -Forestomach hyperplasia (f) -Squamous epithelial hyperplasia of the larynx
200	1500	-Centrilobular hepatocellular hypertrophy (f) -Intrahepatocellular erythrocytes (m) -Multinucleated hepatocytes (m) -Intrahepatocellular erythrocytes (m) -Liver eosinophilic focus (f)
100	740	-Alveolar/bronchiolar epithelial hyperplasia, peribronchiolar fibrosis -Centrilobular hepatocellular hypertrophy (m) -Forestomach inflammation (m)

Newton, *et al.*, 1997: Rat, Subchronic, Inhalation, 4 wk, 6 hr/d, 5 d/wk Tests Completed: Hematology and clinical chemistry, macro and microscopic pathology		
Exposure Levels		**Treatment-Related Effects**
ppm	**mg/m³**	
1044	7700	-Hyperactivity and tremor -Alpha-2u-globulin nephropathy (m)
494	3600	-Increased liver weight -Centrilobular hepatocellular hypertrophy -Altered blood chemistry
262	1900	-Increased activity -Increased kidney weight -Eosinophilic granules in proximal convoluted tubules in kidney (m)
100	740	-No observed effects

Newton, *et al.*, 1997: Rat, Subchronic, Inhalation, 13 wk, 6 hr/d, 5 d/wk Tests Completed: Hematology and clinical chemistry, macro and microscopic pathology, Neuropathology, Motor and functional tests		
Exposure Levels		**Treatment-Related Effects**
ppm	**mg/m^3**	
252	1900	-Increased liver and kidney weight -Centrilobular hepatocellular hypertrophy -Eosinophilic granules in proximal convoluted tubules in kidney (m) -Altered blood chemistry (f)
51, 10	380, 74	-No observed effects

NTP, 1992: Mouse, Subchronic, Oral gavage, 2 wk Tests Completed: Hematology and clinical chemistry; macro and microscopic pathology	
Exposure Levels (mg/kg)	**Treatment-Related Effects**
1000	-Increased liver weight
400	-Hepatocellular hypertrophy -Altered blood chemistry
50, 10	-No observed effects

NTP, 1992: Rat, Subchronic, Oral gavage, 2 wk Tests Completed: Hematology and clinical chemistry; macro and microscopic pathology	
Exposure Levels (mg/kg)	**Treatment-Related Effects**
1000	-Increased kidney weight (f) -Altered blood chemistry and hematology
400	-Increased liver weight (f) -Hepatocellular hypertrophy (f) -Increased kidney weight (m) -Adrenal vacuolation
50	-Increased liver weight (m) -Hepatocellular hypertrophy (m) -Alpha-2u-globulin nephropathy (m)
10	-No observed effects

Macri, et al, 1987: Rat, Subchronic, Oral gavage, 4 wk Tests Completed: Hematology and clinical chemistry; macro and microscopic pathology	
Exposure Levels (mg/kg)	**Treatment-Related Effects**
1000	-Increased salivation -Decreased body weight (m) -Increased liver weight -Adrenal cortex vacuolation (m) -Altered blood chemistry (f)
100	-Increased kidney weight (m) -Hyaline droplet nephrosis (m) -Altered blood chemistry (m)
10	-No observed effects

p-CHLORO-α,α,α-TRIFLUOROTOLUENE

CAS Number: 98-56-6

Synonyms: *p*-chlorobenzotrifluoride (PCBTF); 1-Chloro-4-(trifluoromethyl)benzene

I. PHYSICAL AND CHEMICAL PROPERTIES (HSDB, 2018)

Molecular formula	$C_7H_4F_3Cl$
Molecular weight	180.55 g/mole
Boiling point	138.5 deg C
Melting point	-33 deg C
Vapor pressure	7.63 mm Hg (25 deg C)
Liquid density	1.33 g/mL (25 deg C)
Log octanol/water partition coefficient	3.60 (25 deg C) (estimated)
Water solubility	29 mg/L (25 deg C)
Air concentration conversion	1 ppm = 7.38 mg/m^3

Structurally, PCBTF consists of a benzene ring substituted with the electron-withdrawing groups, chlorine and trifluoromethyl. Both these substituents deactivate the aryl ring with respect to electrophilic attack (and oxidation). In addition, the carbon-fluorine bond of the trifluoromethyl group is less prone to chemical or enzymatic attack than the carbon-hydrogen bond of a methyl group.

PCBTF has a vapor pressure and boiling point that are similar to that of the xylene isomers and ethylbenzene. Table 1 shows a comparison of these properties for several common petroleum-based solvents.

Table 1. PCBTF vapor pressure (VP) and boiling point (BP) comparison with selected solvents		
Solvent	VP (mm Hg, 25 deg. C)	BP
Benzene	94.8	80.0
Toluene	28.4	110.6
Ethylbenzene	9.6	136.2
p-Xylene	8.8	138.3
m-Xylene	8.3	139.1
PCBTF	**7.6**	**138.5**
o-Xylene	6.7	144.5

PCBTF has a low water solubility and its log octanol/water partition coefficient of 3.6 indicates that it partitions preferentially into organic liquid phases: the ratio of PCBTF

concentrations in this two-phase system at equilibrium would be about 4000 in favor of octanol.

II.   HEALTH ASSESSMENT VALUES

Unit Risk Factor $(\mu g/m^3)^{-1}$	8.6×10^{-6}
Slope Factor $(mg/kg\text{-}day)^{-1}$	3.0×10^{-2}

The values are based on data from a recent National Toxicology Program (NTP) study (NTP, 2018) where an elevated incidence of liver tumors was observed in male B6C3F1 mice exposed to PCBTF by inhalation. For dose-response calculations, OEHHA used US EPA's Benchmark Dose Software (BMDS) (US EPA, 2017) and its implementation of the multi-stage cancer model (including linear low-dose extrapolation).

III.   CARCINOGENICITY

Currently, there are four peer-reviewed cancer studies of PCBTF exposure in experimental animals available for use in a cancer hazard and dose-response evaluation: the toxicology and carcinogenesis rat and mouse (both male and female for each species) studies reported by NTP (2018). These studies are described in the next section.

NTP Carcinogenicity Bioassay

The NTP (2018) toxicology and carcinogenesis studies exposed female and male B6C3F1 mice and both sexes of Hsd:Sprague Dawley SD rats, in groups of 50, to PCBTF by inhalation 6.2 hours/day, 5 days/week for 104-to-105 weeks. Mice were exposed to concentrations of 100, 200, or 400 ppm (738, 1476, or 2952 mg/m^3) and rats to 100, 300, or 1000 ppm (738, 2214, 7380 mg/m^3). The animals were between 5 and 6 weeks old at the beginning of exposure.

The purity of the PCBTF used in the study was determined to be greater than 99.5%, containing small amounts of the 3-chloro, and 2-chloro isomers as impurities. Analysis of the chamber atmosphere during exposure indicated that 3-chlorobenzotrifluoride and 2-chlorobenzotrifluoride were present at 0.3% and 0.2%, respectively.

The general status and body weight of the animals were monitored during the study. Upon death, animals were necropsied and histopathologic examination of all relevant tissues (more than 40 sites) was performed on all animals. Statistics on mortality

throughout the study were tabulated and presented in the form of Kaplan-Meier survival curves. Copies of these graphs are provided in Attachment 1.

The NTP (2018) report identified significant increases in tumor incidence based upon Poly-3 adjusted statistical tests. Pairwise comparisons of dosed groups with control groups were made and dose-related trends were evaluated. These results are discussed in the following sub-sections.

<u>Neoplasms in Mice</u>

The significant results observed for mice in the NTP study are shown in Table 2.

A dose-related, significant increase in the rate of liver tumors (hepatocellular adenoma and carcinoma, and hepatoblastoma) was seen in both female and male mice. Statistical tests generally produced *p*-values of <0.01 at the highest exposure level of 400 ppm (3000 mg/m^3) and for the overall dose-response trends. In the males, the incidence of hepatocellular carcinoma was elevated at 100 ppm (740 mg/m^3) and 400 ppm (3000 mg/m^3), as well as for hepatoblastoma at 400 ppm.

Table 2. Un-adjusted tumor incidence in mice exposed to PCBTF by inhalation (NTP, 2018) [a,b]								
Tumor type	**Incidence by concentration**				**Statistical p-values for pairwise comparison with controls** (p-value for trend in control column)			
ppm	**0**	**100**	**200**	**400**	**0**	**100**	**200**	**400**
mg/m^3	**0**	**740**	**1500**	**3000**	**0**	**740**	**1500**	**3000**
(Female mouse)								
Harderian Gland: Adenoma	2/50*	6/50	6/50	8/50*	0.049	0.134	0.134	0.046
Harderian Gland: Adenocarcinoma	0/50	0/50	3/50	0/50	0.453	1.000	0.121	1.000
Harderian Gland: Adenoma or Adenocarcinoma	2/50*	6/50	9/50*	8/50*	0.047	0.134	0.026	0.046
Liver: Hepatocellular Adenoma	12/50**	14/50	24/50*	34/50**	<0.001	0.410	0.011	<0.001
Liver: Hepatocellular Carcinoma	7/50**	8/50	12/50	34/50**	<0.001	0.500	0.154	<0.001
Liver: Hepatoblastoma	0/50**	0/50	1/50	8/50**	<0.001	1.000	0.500	0.003
Liver: Hepatocellular Adenoma, Hepatocellular Carcinoma, or Hepatoblastoma	18/50**	18/50	29/50*	46/50**	<0.001	0.582	0.022	<0.001
(Male mouse)								
Liver: Hepatocellular Adenoma	25/50	24/50	31/50	29/50	0.152	0.655	0.157	0.274
Liver: Hepatocellular Adenoma (multiple)	9/50**	15/50	19/50*	21/50**	0.006	0.121	0.022	0.008
Liver: Hepatocellular Carcinoma	8/50**	19/50*	16/50	35/50**	<0.001	0.012	0.050	<0.001
Liver: Hepatoblastoma	1/50**	1/50	1/50	15/50**	<0.001	0.753	0.753	<0.001
Liver: Hepatocellular Adenoma, Hepatocellular Carcinoma, or Hepatoblastoma	31/50**	37/50	40/50*	48/50**	<0.001	0.142	0.038	<0.001

(a) The numerator represents the number of tumor-bearing animals; the denominator represents animals examined microscopically (for liver), or the number of animals necropsied (for Harderian gland).

(b) * = $p<0.05$, ** = $p<0.01$; p-value indicators are from pairwise comparisons with controls using Fisher exact tests performed by OEHHA; p-values in the control column are for a Cochran-Armitage trend tests performed by OEHHA.

Although hepatocellular adenomas were not significantly elevated in male mice, the occurrence of multiple adenomas was significantly increased at the 200 (1500 mg/m^3) ($p<0.05$) and 400 ppm ($p<0.01$) exposure levels and a significant dose-related trend was demonstrated ($p<0.01$)

In the females, there were increased rates of hepatocellular adenoma at 200 ppm, (1500 mg/m^3) and above, hepatocellular carcinoma at 400 ppm (3000 mg/m^3), and hepatoblastoma at 400 ppm.

The incidence of liver tumors combined (i.e., the presence of hepatocellular adenomas or carcinomas, or hepatoblastomas) was also significantly elevated in both the males and females at 200 ppm (1476 mg/m^3) and the highest dose. As noted above, significant trends ($p<0.01$) were also found.

The incidence of Harderian gland adenoma in female mice appeared to be elevated at the 400 ppm (3000 mg/m^3) exposure level ($p<0.05$). The Harderian adenomas also displayed a significant dose-related trend ($p<0.05$). Finally, the incidence of combined Harderian gland adenomas and adenocarcinomas in females was elevated at 200 ppm and greater ($p<0.05$), and a significant trend ($p<0.05$) was observed. (The Harderian gland is an exocrine gland located in the ocular orbital of rodents. Although humans do not have this type of gland, tumor data from this tissue may be used in assessing cancer risk in humans because tumor-site concordance is not expected across species.)

<u>Neoplasms in Rats</u>

The notable tumor-incidence data for rats are presented in Table 3.

Table 3. Un-adjusted tumor incidence in rats exposed to PCBTF by inhalation (NTP, 2018) [a,b]								
Tumor type	**Incidence by concentration**				**Statistical p-values for pairwise comparison with controls** (p-value for trend in control column)			
ppm	**0**	**100**	**300**	**1000**	**0**	**100**	**300**	**1000**
mg/m³	**0**	**738**	**2214**	**7380**	**0**	**738**	**2214**	**7380**
(Female rat)								
Adrenal Medulla: Benign Pheochromocytoma	0/49	3/50	4/50	6/50*	0.022	0.125	0.061	0.014
Adrenal Medulla: Benign or Malignant Pheochromocytoma	0/49	4/50	4/50	6/50*	0.037	0.061	0.061	0.014
Thyroid Gland (C-cell): Adenoma	2/50**	8/50*	8/50*	14/50**	0.002	0.046	0.046	0.001
Thyroid Gland (C-cell): Adenoma or Carcinoma	2/50**	10/50*	8/50*	15/50**	0.003	0.014	0.046	<0.001
Uterus: Stromal Polyp	7/50	9/50	16/50*	12/50	0.164	0.393	0.028	0.154
Uterus: Stromal Polyp or Stromal Sarcoma	7/50	9/50	17/50*	12/50	0.171	0.393	0.017	0.154
Uterus: Adenocarcinoma	1/50**	1/50	0/50	5/50	0.010	0.753	1.000	0.102
(Male rat)								
Lung: Alveolar/bronchiolar Adenoma or Carcinoma [(c)]	*0/50*	*2/50*	*0/50*	*3/50*	0.072	0.247	1.000	0.121
Thyroid Gland (C-cell): Adenoma	2/50**	5/49	3/49	12/50**	0.001	0.210	0.490	0.004
Thyroid Gland (C-cell): Adenoma or Carcinoma	3/50**	5/49	4/49	13/50**	0.001	0.346	0.489	0.006

(a) The numerator represents the number of tumor-bearing animals; the denominator represents animals examined microscopically (for adrenal gland, lung, and thyroid gland), or the number of animals necropsied (for uterus).

(b) * = p<0.05, ** = *p*<0.01; *p*-value indicators are from pairwise comparisons with controls using Fisher exact tests performed by OEHHA; p-values in the control column are for Cochran-Armitage trend tests performed by OEHHA.

(c) Tumor type and incidence in italics: equivocal finding of carcinogenicity by NTP (2018).

A significant increase in thyroid C-cell adenoma or adenoma and carcinoma incidence was observed for female rats at all PCBTF exposure levels, along with a significant dose-response trend (p<0.01). Significant increases in thyroid C-cell adenoma or adenoma and carcinoma incidence were observed for male rats at 1000 ppm (7400 mg/m^3) (*p*<0.01), along with a significant dose-related trend (*p*<0.01).

In female rats, elevated tumor incidence was observed in the adrenal medulla, where the rate of benign adrenal pheochromocytoma was significantly elevated (*p*<0.05) at 1000 ppm (7400 mg/m^3). The incidence of uterine stromal polyps was elevated (*p*<0.05) in female rats exposed to PCBTF at 300 ppm (2200 mg/m^3). These tumors were also elevated at 1000 ppm (7400 mg/m^3) but the increase was not statistically significant. A uterine stromal sarcoma was also observed in the 300 ppm exposure group. Adenocarcinoma of the uterus displayed a significant dose-response trend (*p*<0.01), although pairwise comparisons with the controls did not reach significance. Atypical endometrial hyperplasia was also seen in several animals at 300 and 1000 ppm (2200 and 7400 mg/m^3).

Finally, in the males, a nearly significant increase of alveolar-bronchiolar adenoma or carcinoma was observed: *p*-values of 0.073 and 0.086 were found for the trend test and the high-dose comparison, respectively. NTP concluded that these tumors could have been treatment-related, considering that the background incidence of lung tumors in Hsd:Sprague-Dawley SD rats is likely to be low.

Toxicokinetics

Information on the absorption, distribution, metabolism, and excretion of PCBTF in mammals is not abundant. However, several toxicokinetics studies in rats have been published. The available data indicate that PCBTF is:

- Readily absorbed, both orally and by inhalation;

- Widely distributed throughout the body with a tendency to concentrate in fat and fatty tissues;

- Primarily excreted unchanged via exhalation;

- Secondarily metabolized via aromatic hydroxylation, and excreted through urine and feces as conjugated phenolic compounds; and,

- Converted in small amounts to mercapturic acid metabolites.

In one metabolism study, Quistad and Mulholland (1983) exposed two male Sprague-Dawley rats to a single gavage dose of one mg/kg, and six female Sprague-Dawley rats to either one or 104 mg/kg of ^{14}C-trifluoromethyl, radio-labelled PCBTF (15.1

millicuries per millimole). Table 4 presents a summary of radiolabel-balance measurements presented by the authors.
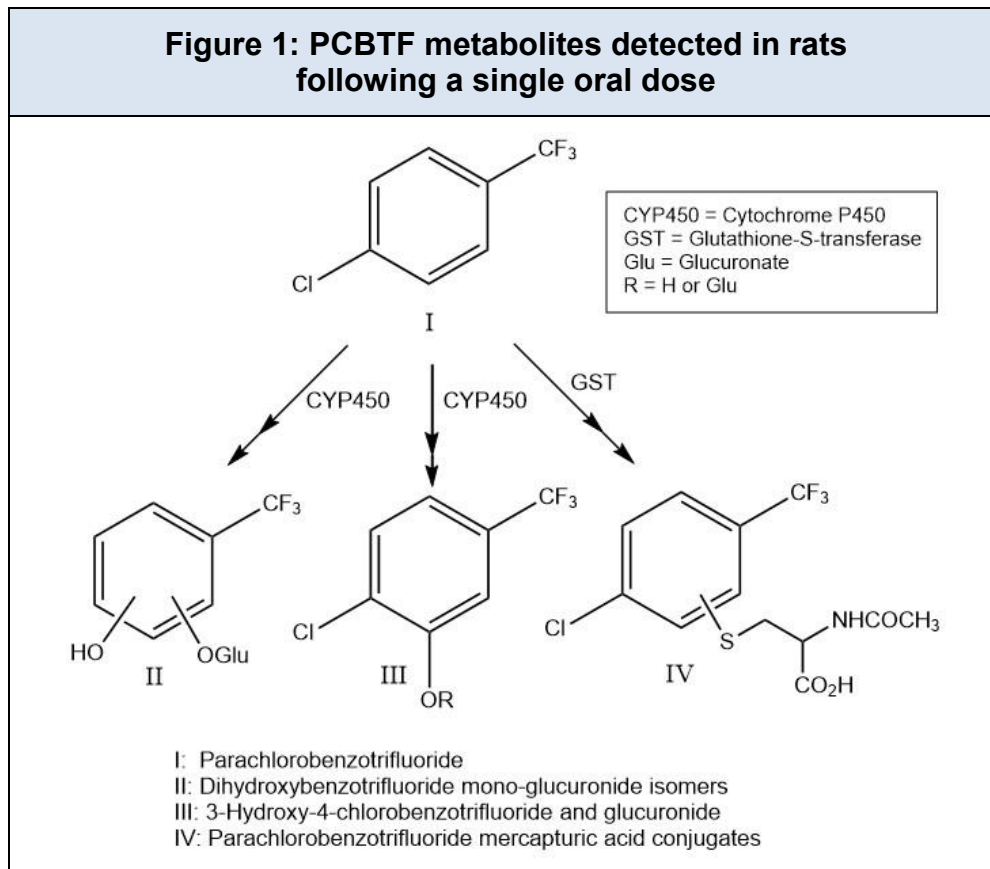
Table 4: Percent of radioactivity recovered from rats given a single oral dose of labelled PCBTF (Quistad and Mulholland, 1983)			
Sex:	Female[a]	Female[b]	Male[b]
Oral dose (mg/kg):	1	104	1
	Percent recovered		
Urine	13.6	5.9	14.9
Feces:	2.6	2.2	3.5
--Methanol extract	2.3	2.0	3.0
--Residual solids	0.3	0.2	0.5
Carcass:	1.2	0.19	0.18
--Methanol and chloroform extracts	1.1	0.17	0.16
--Residual solids	0.07	0.02	0.02
$^{14}CO_2$	<0.03	--	--
Volatile organics (PCBTF)	62	82	68
Total recovery	79	90	87

(a) Average for four rats; (b) Average for two rats.

Briefly, after four days of monitoring, 62 to 68 percent of the lower dose, and 82 percent of the higher dose were exhaled unchanged. Excretion of radio-labelled substances in urine and feces at the lower dose represented 13.6 to 14.9 percent and 2.6 to 3.5 percent of the applied dose, respectively. The higher-dose females excreted 5.9 percent of the radiolabel in urine and 2.2 percent in feces. One percent or less of the dose was recovered in the carcasses, and total recovery of the radiolabel was 79 to 90 percent. The authors noted that total recovery of the administered dose was hindered by the volatility of PCBTF.

The main urinary metabolites were the glucuronide conjugates of 4-chloro-3-hydroxybenzotrifluoride and 3,4-dihydroxybenzotrifluoride, measured at 7.1 percent of the dose in low-dose females and 3.5 percent in males. Unconjugated 4-chloro-3-hydroxybenzotrifluoride was also found at 0.5 percent of the dose in the urine of the male rats (females not sampled). These hydroxylated metabolites are likely generated via initial cytochrome P450 (CYP450) oxidation of PCBTF (although Quistad and Mulholland did not attempt to identify the specific enzymes involved). Small amounts of mercapturic acid metabolites, 0.2 percent or less, were also

measured in all groups. Figure 1 presents a metabolic scheme developed by OEHHA based on the above findings. (In the scheme, OEHHA assumed that aryl ring oxidation of PCBTF to produce metabolites II and III occurs via the initial action of one or more isoforms of CYP450.)

Figure 1: PCBTF metabolites detected in rats following a single oral dose

CYP450 = Cytochrome P450
GST = Glutathione-S-transferase
Glu = Glucuronate
R = H or Glu

I: Parachlorobenzotrifluoride
II: Dihydroxybenzotrifluoride mono-glucuronide isomers
III: 3-Hydroxy-4-chlorobenzotrifluoride and glucuronide
IV: Parachlorobenzotrifluoride mercapturic acid conjugates

Quistad and Mulholland (1983) also analyzed residual concentrations of PCBTF four days after exposure. Levels found in the fat of the female rats were relatively high when compared to other tissues. For example, in the low-dose females, mean concentrations in parts per billion (ppb) were as follows: abdominal fat (104), lungs (12), kidney (6), and liver (1). The male rats appeared to concentrate less PCBTF in fat, where concentrations for the same tissues as above were, respectively: 6, 6, 2, and 2 ppb.

NTP carried out toxicokinetic experiments in a small number of F344/N rats as part of a larger toxicology study (NTP, 1992). Male rats (two or three per group) were administered 4.7 mg/kg PCBTF dissolved in aqueous "Tween 80" solution via tail-vein injection, or else were given a single oral-gavage dose of 10, 50, or 400 mg/kg. The vehicle for gavage-dosing was either corn oil or α-cyclodextrin. Use of α-cyclodextrin resulted in a shorter time to maximum blood level and a higher

absorption rate. However, total absorption and the area under the concentration curve (AUC) were not affected by the choice of vehicles.

The biological half-life of PCBTF in venous blood was estimated to be 19 hours. Oral absorption appeared to be 100 percent at all three dose levels, with an absorption half-life between 0.8 and 2.3 hours (faster absorption was observed at lower doses). The NTP (1992) study also noted that upon repeated dosing over 14 days, PCBTF concentrations in the blood and liver of male and female rats were similar, although the males had much higher kidney concentrations than the females.

Newton *et al.* (1998) conducted an inhalation toxicity study of PCBTF that included measurements of blood and tissue concentrations in 15 groups of three female Sprague-Dawley rats exposed for up to six hours to 53 ppm (390 mg/m^3) of PCBTF, and then followed, post-exposure, for up to 24 hours. (The rats had been exposed to 51 ppm (380 mg/m^3) for 6 hours per day, 5 days per week, for 13 weeks prior to this test). As was seen with oral exposure, PCBTF displayed a tendency to concentrate in the fat of females. For example, 24 hours post-exposure, fat contained 142 ppm PCBTF, whereas lung, kidney and liver concentrations averaged, respectively, 7.1, 4.1, and 2.5 ppm.

In a companion study looking at CYP450 enzyme-induction, Pelosi *et al.* (1998) obtained the livers from four groups of 10 male and 10 female Sprague-Dawley rats from Newton *et al.* (1998), that had been exposed by inhalation to 0, 10, 51, or 252 ppm (0, 74, 380, or 1900 mg/m^3) of PCBTF for 13 weeks (6 hours per day, 5 days per week). Post-exposure activities of several CYP isozymes were determined in microsomes prepared from the livers by measuring the transformation rates of chemicals that are known to be preferentially metabolized by specific CYPs (e.g., chlorzoxazone hydroxylation by CYP 2E1).

Moderate increases of metabolic activity, approximately two-fold, were found for CYP 1A1/2, 2B1/2 (in females), 2E1 (in males), and 3A1/2 (in females) at the highest exposure level. Male liver microsomes displayed a five-fold increase in CYP 2B1/2 activity. No increases in enzymatic activity were seen for CYP 3A in males and CYP 2E1 in females.

In a second related study, Knaak *et al.* (1998) used the liver microsomes prepared by Pelosi *et al.* (1998) to estimate the Vmax and Km values for enzymatic conversion of PCBTF to 3-hydroxy-4-chlorobenzotrifluoride, but did not observe a significant increase in liver metabolism in the more highly exposed rats.

Physiologically-Based Pharmacokinetic (PBPK) Model

A PBPK model for PCBTF inhalation exposure to rats and humans was developed by Knaack *et al.* (1998; 1995). The model included compartments for liver, brain, fat, kidney, and slowly and rapidly perfused organs. The metabolism of PCBTF was represented by model components for:

- CYP450 oxidation of PCBTF in the liver;

- Formation of glucuronide conjugates of the phenolic metabolites produced by oxidation; and

- Formation of glutathione conjugates.

Tissue-blood and blood-air partition coefficients were estimated for rats and humans *in vitro*. Metabolic constants (V_{max} and K_m) for the oxidation of PCBTF in rats were also determined *in vitro*, using hepatic microsomal protein. Constants for the conjugation reactions were chosen to be consistent with the metabolite ratios in orally exposed rats, as reported by Quistad and Mulholland (1983). Metabolic constants for the human model were estimated by weight-scaling of the rat data.

The model's predictions were compared to data collected by Newton *et al.* (1998), where blood and tissue concentrations were measured in female rats exposed to approximately 50 ppm (370 mg/m^3) of PCBTF for six hours after 13 weeks of daily exposure at this concentration. No additional inhalation studies reporting on blood or tissue concentrations were available for model calibration or validation.

Based upon results graphically presented by Knaak *et al.* (1998), the rat model appeared to be moderately successful at predicting blood, liver, and fat concentrations of PCBFT during the 6 hours of exposure to 50 ppm, but became increasingly inaccurate in the post-exposure period. For example, at 24 hours post-exposure, the concentration in fat predicted by the model was about 10 times lower than the concentration measured by Newton *et al.* (1998). Also, the predicted liver concentration was about 5 times lower than the measured value at this point.

OEHHA judged the model to be incomplete for the purposes of the dose-response analysis for several reasons:

- Inadequate model validation: The only *in vivo* blood and tissue data available to verify the model output was from a single exposure concentration in female rats.

- The blood and tissue concentrations of PCBTF predicted by the rat model appeared to deviate substantially from the experimental data during post-

exposure periods.

- The authors did not demonstrate whether the rat model could adequately simulate blood and tissue concentrations at exposure levels other than 50 ppm.

- The human model was not based on experimentally derived metabolic constants, nor was it tested against experimental data.

- The authors did not develop a mouse model.

Nonetheless, the PBPK model does provide some toxicokinetic information for rats exposed by inhalation. In particular, the model output indicates that female rats exposed one time for 6 hours to 50 ppm would exhale 83 percent of the absorbed PCBTF unchanged, and metabolize 8.4 percent of the dose. Residual concentrations in fat and slowly perfused tissues were respectively estimated at 4.4 and 3.7 percent of the dose (presumably after 24 hours, though not stated in the paper).

However, it should also be noted that the PBPK model only uses liver metabolism to estimate parent compound concentrations. It does not include components for the formation and elimination of electrophilic intermediates (e.g., epoxides and quinones) in the liver. Additionally, although it includes equations for the formation of the phenolic metabolites, it does not include equations for their elimination (e.g., via urine and bile). The latter would be needed to determine blood/organ concentrations of these metabolites.

Epidemiological Studies

No studies of cancer risk to humans resulting from PCBTF exposure were found in the literature.

Genotoxicity

Genotoxicity data for PCBTF come from several peer-reviewed studies as well as a number of non-peer-reviewed industry reports that were submitted to US EPA as part of a regulatory process under the Toxic Substances Control Act. Data from these studies are summarized in Table 5. The assays included appropriate negative, solvent and positive controls.

Table 5: PCBTF Genotoxicity Data				
Test System	**Concentration**	**Results**		**Reference**
		-S9	**+S9**	
DNA damage and repair				
Unscheduled DNA synthesis; human embryonic epithelial cells	0.2 to 10 µl/ml	+	NT	Benigni *et al.* (1982)
Rec-assay; *B. subtilis* (PB 1652, PB 1791)	500 to 10,000 µg/disk	-	NT	Mazza *et al.* (1986)
DNA repair deficiency; *E. coli* (W3110 polA+, P3478 polA-)	0.01 to 10 µl/plate	-	-	Litton Bionetics (1978a)*
Gene mutation				
Ames reverse mutation; *S. typhimurium* (TA98, 100, 1535, 1537, 1538)	100 to 2500 µg/plate	-	-	Mazza *et al.* (1986)
Ames reverse mutation; *S. typhimurium* (TA98, 100, 1535, 1537, 1538), *S. cerevisiae* (D4)	0.01 to10 µl/plate	-	-	Litton Bionetics (1978a)*
Ames reverse mutation; *S. typhimurium* (TA98, 100, 1535, 1537)	0.1 to 0.4 µl/plate	-	-	Benigni *et al.* (1982)
Ames reverse mutation; *S. typhimurium* (TA98, 100, 1535, 1537)	10 to 1,000 µg/plate	-	-	Haworth *et al.* (1983)
Ames reverse mutation; *S. typhimurium* (TA98, TA100), *E. coli* (strain WP2 uvrA/pKM101)	10 to 6,000 µg/plate	-	-	NTP (2018)
Ames reverse mutation; *S. typhimurium* (TA1535, TA1537, TA98, TA100) tested with urine from exposed male CD-1 mice	50, 167 or 500 mg/kg (gavage, 2 days)	-	NA	Litton Bionetics (1979a)*
Forward mutation; *S. typhimurium* (TA1535 and TA100)	50 to 150 µg/plate	-	NT	Bignami and Crebelli (1979)
Forward mutation; L5178Y mouse lymphoma cells	3.13 to 50 nl/ml	-	-	Litton Bionetics (1978b)*
Chromosomal damage				
Mitotic recombination; *S. cerevisiae* (6117)	2000 µg/ml	-	-	Mazza *et al.* (1986)
Mitotic recombination; *A. nidulans*	0.25 to 2.5 µl/plate	-	NT	Benigni *et al.* (1982)

Table 5: PCBTF Genotoxicity Data				
Test System	**Concentration**	**Results**		**Reference**
		-S9	**+S9**	
Sister chromatid exchanges; L5178Y mouse lymphoma cells	0.0025 to 0.04 µl/ml	**+**	**+**	Litton Bionetics (1979b)*
Chromosomal aberrations; Chinese hamster ovary cells	30 to 130 nl/ml	**-**	**-**	Lilly Research Laboratories (1983)*
Chromosomal aberrations; *in vivo* Sprague-Dawley male, female rat – bone marrow cells	0.5, 1.7 or 5 ml/kg (single gavage dose)	**-**	NA	Lilly Research Laboratories (1983)*
Micronucleus formation; *in vivo* Sprague-Dawley male, female rat – peripheral blood	125 to 2000 ppm (inhalation, 14 weeks)	**-**	NA	NTP (2018)
Micronucleus formation; *in vivo* B6C3F1/N male, female mice – peripheral blood	125 to 2000 ppm (inhalation, 14 weeks)	**+**[†]	NA	NTP (2018)
Morphological cell transformation				
Balb/3T3 mouse cells	0.1 to 40 nl/ml	**-**	NT	Litton Bionetics (1980)*
Balb/3T3 mouse cells	10 to 300 µg/ml	**-**	**-**	Lilly Research Laboratories (1983)*

(-S9): without metabolic activation; (+S9): with metabolic activation
(**+**): positive result; (**-**): negative result
NT: not tested; NA: not applicable
(*): non-peer-reviewed report; (†): for males only

DNA damage and gene mutation assays using bacterial and yeast systems, most of which employed a metabolic activation system containing liver microsomal (S9) preparations from Aroclor-induced rats, reported negative findings. Chromosomal damage assays in yeast were also negative. Conversely, *in vitro* and *in vivo* mammalian chromosomal damage studies showed mixed results and a mammalian unscheduled DNA synthesis (UDS) assay reported positive results. Of the three *in vivo* genotoxicity bioassays for PCBTF, two tested negative for chromosomal aberrations while one tested positive. Rats tested negative for increases in micronucleus formation in peripheral blood cells, and for chromosomal aberrations in bone marrow cells. On the other hand, a test of peripheral blood cells from male mice exposed to 2000 ppm (15,000 mg/m^3) for 14 weeks showed an increase in micronucleus formation. Overall, the genotoxicity test data provide limited evidence that PCBTF is genotoxic.

It should be noted that two of the more sensitive genotoxicity assays, namely the

"single-cell, gel electrophoresis" (comet) test for DNA-strand breaks and tests measuring oxidative DNA damage or DNA-adduct formation, have apparently not been completed for PCBTF or its metabolites. This represents a data gap in the PCBTF genotoxicity database. Additional details of the genotoxicity assays are provided in the following sub-sections.

<u>DNA damage and repair</u>

Only one of the three studies that evaluated PCBTF-induced DNA damage and repair reported positive results. PCBTF tested positive for induction of UDS at relatively high concentrations of 0.2 to 10 microliters per milliliter (µl/ml) with a clearly defined dose-dependent response up to 2 µl/ml in human embryonic epithelial cell cultures (Benigni *et al.*, 1982). However, PCBTF failed to induce DNA damage in the rec-assay in *B. subtilis* (strains PB 1652 and PB 1791) at concentrations of 500 to 10,000 micrograms per disk (µg/disk) (Mazza *et al.*, 1986). PCBTF also tested negative in an assay that detects DNA damage induced by chemical exposure via selective killing of indicator strains lacking different DNA repair systems. This DNA repair deficiency assay was conducted in *E. coli* indicator strains W3110 polA+ and P3478 polA- in the presence and absence of metabolic activation, at concentrations of 0.01 to 10 µl per plate (Litton Bionetics, 1978a, unpublished).

<u>Gene mutation</u>

All studies of PCBTF mutagenicity have reported negative findings. PCBTF tested negative in the 8-azaguanine (8-AG) resistance test, a forward mutation assay that selects induced 8-AG resistant mutants, in *S. typhimurium* (strains TA1535 and TA100) at concentrations of 50 to 150 µg/plate (Bignami and Crebelli, 1979). Similarly, there was no increase in mutant frequency at the thymidine kinase (TK) locus in the L5178Y mouse lymphoma forward mutation assay at PCBTF concentrations of 3.13 to 50 nl/ml with or without metabolic activation (Litton Bionetics, 1978b, unpublished).

When tested either directly or in the presence of metabolic activation, PCBTF failed to demonstrate mutagenic activity as assessed by the Ames reverse mutation assay using *S. typhimurium* (strains TA98, TA100, TA1535, TA1537, and TA1538), and similar assays using E. coli strain WP2 uvrA/pKM101 and S. cerevisiae strain D4 (Litton Bionetics, 1978a, unpublished; Benigni *et al.*, 1982; Haworth *et al.*, 1983; NTP, 2018). PCBTF was also found to be inactive for mutagenicity in a host-mediated *in vitro* assay in which urine collected from male CD-1 mice exposed to 50, 167 or 500 mg/kg by oral gavage for 2 days was tested in *S. typhimurium* strains TA1535, TA1537, TA98, and TA100 (Litton Bionetics, 1979a, unpublished).

Pretreatment of the collected urine with the deconjugating enzyme beta-glucuronidase did not alter the results.

<u>Chromosomal damage</u>

Yeast assays

PCBTF did not demonstrate recombinogenic activity in yeast assays when tested directly or in the presence of metabolic activation (Mazza *et al.*, 1986). PCBTF recombinogenic activity, namely mitotic crossing-over (reciprocal recombination) and mitotic gene conversion (non-reciprocal recombination), was tested in the mitotic segregation assay in *S. cerevisiae* strain 6117 at 2000 µg/ml. Similarly, no induction of mitotic crossing-over was observed in *A. nidulans* at PCBTF concentrations of 0.25 to 2.5 µl/plate (Benigni *et al.*, 1982).

Mammalian assays

Studies on chromosomal damage induced by PCBTF have produced mixed results in mammalian cells. In L5178Y mouse lymphoma cells, PCBTF tested positive for induction of sister chromatid exchange (SCE) both directly and in the presence of metabolic activation (Litton Bionetics, 1979b, unpublished). At all five concentrations tested between 0.0025 and 0.04 µl/ml, PCBTF significantly increased the frequency of SCE/chromosome when tested directly, with SCE frequency generally increasing with dose. With metabolic activation, however, three of five concentrations (including the lowest but not highest) significantly increased SCE frequency relative to that of control. Thus, PCBTF induction of SCE with activation did not demonstrate a clearly defined dose-response trend.

Tests for induction of chromosomal aberrations by PCBTF have been negative *in vitro* and *in vivo* (Lilly Research Laboratories, 1983, unpublished). The *in vitro* study was conducted in Chinese hamster ovary cells at PCBTF concentrations of 30 to 130 nl/ml with metabolic activation and at 30 to 80 nl/ml without activation. For the *in vivo* assay, bone marrow cells from male and female Sprague-Dawley rats were analyzed following administration of a single gavage dose of PCBTF at 0.5, 1.7 or 5 ml/kg.

The frequency of micronucleated cells was evaluated *in vivo* in peripheral blood of male and female Sprague-Dawley rats and B6C3F1/N mice exposed to PCBTF at concentrations of 125 to 2000 ppm (923 to 14,760 milligrams per cubic meter [mg/m^3]) by inhalation for a duration of 6 hours/day for 5 days/week for 14 weeks (NTP, 2018). Whereas no induction of micronucleus formation was observed in rats, PCBTF did induce a small, statistically significant increase in the frequency of micronucleated cells in male and female mice at the highest concentration of 2000 ppm. NTP considered this effect to only be biologically significant in males because

the observed values for the female mice were within historical control ranges

Morphological cell transformation

The Balb/3T3 mouse cell assay is routinely used for evaluation of the carcinogenic potential of chemical agents *in vitro*, as determined by the ability of the test chemical to induce foci of transformed cells that are super-imposed on the monolayer of normal cells in culture. In this assay, PCBTF did not induce the appearance of transformed cells when tested directly at concentrations of 0.1 to 40 nanoliters per milliliter (nl/ml) (Litton Bionetics, 1980, unpublished) or 10 to 300 μg/ml (Lilly Research Laboratories, 1983, unpublished), or with metabolic activation at concentrations of 10 to 300 μg/ml (Lilly Research Laboratories, 1983, unpublished).

IV.   CANCER HAZARD SUMMARY

The NTP (2018) study was a well-designed and implemented lifetime animal study carried out in both sexes of B6C3F1/N mice and Hsd:Sprague Dawley SD rats. The study indicated that lifetime exposure to PCBTF via inhalation can produce significantly elevated incidence of various tumor types in the following tissues:

Mouse	Female	Harderian gland and liver
	Male	Liver
Rat	Female	Adrenal gland, thyroid gland and uterus
	Male	Lung (equivocal) and thyroid gland

Information from the toxicokinetic studies discussed above indicates that PCBTF is readily absorbed in rats, and that a portion of the absorbed dose is subject to oxidative metabolism, potentially giving rise to reactive and genotoxic metabolic intermediates. The toxicokinetics of PCBTF in humans are likely to be broadly similar to that observed in the rat. In addition, the available genotoxicity test data provides limited evidence that PCBTF is genotoxic.

On June 28, 2019, OEHHA listed PCBTF as a substance "known to the state to cause cancer" under Proposition 65 (OEHHA, 2019), based on NTP's formal identification of the chemical as a carcinogen. At the time of writing, neither the International Agency for Research on Cancer (IARC) nor US EPA have evaluated the cancer hazard potential of PCBTF.

V.   QUANTITATIVE CANCER RISK ASSESSMENT

Adjustments for Differential Early-Mortality

Early deaths in a lifetime cancer study reduce the number of animal-days of exposure that pose a risk of developing tumors. Significant differences in survival among

exposure groups sometimes occur as a result of early non-tumor-related deaths in the more highly exposed animals (i.e., deaths that result from causes other than the specific tumor of interest). In these instances, using the number of animals that were initially entered into a study to calculate tumor incidence can underestimate risk at the higher doses. In order to obtain a more accurate estimate of the dose-response relationship, the crude incidence rates are therefore adjusted prior to carrying out statistical tests or estimating dose-response functions. OEHHA adjusted the tumor incidence for PCBTF as follows.

Survival of female and male mice in all the exposed groups was similar to survival in the control groups prior to week 85. (OEHHA defines "similar" as a difference in mortality of less than 15 percent prior to week 85 of a two-year study). Under these circumstances, OEHHA's practice is to adjust the number of animals-at-risk using the "effective number" procedure: The effective number of animals in an exposure group is the number alive at the time of first occurrence of the tumor of interest, as observed in any of the study groups (Gart, *et al.*, 1986). Using the effective number in the denominator of the incidence proportion removes animals that died before they are considered at risk for tumor development, and adjusts for differences in intercurrent mortality among the exposure groups. The method assumes that the animals dying early would have displayed the same tumor-incidence (had they lived to the end of the study) as those animals that survived to the end.

Compared to the mice, the survival patterns of the exposed rats diverged more significantly from their respective control groups. Survival of the most highly exposed male rats was about 15 to 20 percent lower than controls near week 85. Most of the early deaths were due to nephropathy. The survival of the high-dose females also deviated more from the control group after week 75, but in the opposite direction (i.e., the exposed group had less mortality than the controls).

In such cases, where the incidence data could be confounded by larger differences in early deaths, OEHHA typically adjusts the number of animals-at-risk using the "poly-3" method (Portier and Bailer, 1989).[3] Like the effective-number method, the poly-3 procedure modifies the denominator of the incidence rate to account for intercurrent mortality. Animals living for the entire study period are fully included in the denominator, as are those dying early with the tumor of interest. For animals dying

---

[3] In cases with more significant early deaths in the higher-dose groups, OEHHA has also used a multistage Weibull (i.e., "time-to-tumor") model.

early without the tumor of interest, a fractional amount is added to the denominator according to the following equation (for a 2-year study):

Use of the cubic term is based upon the observation that the rate of tumor incidence in rodents over a lifetime increases as a third-order (or fourth-order) function of time (Portier and Bailer, 1989). OEHHA evaluated the rat data using the poly-3-adjusted incidence proportions and statistical test results that were provided in the NTP report.

Choice of Tumor Data to Model

$$\text{Contribution to denominator} = \left(\frac{\text{Time in study}}{2 \text{ years}}\right)^3$$

The incidence of related neoplasms at a tumor site is the preferred datum for use in cancer assessments, per OEHHA's cancer guidelines: "Tumor types considered to represent different stages of progression following initiation of a common original normal cell type are combined, whereas tumor types having different cellular origins are generally not combined..." (OEHHA, 2009). When combining tumor types, OEHHA generally follows NTP's recommendations, as well as those of Brix, Hardisty, and McConnell (2010).

The dose-response assessment was carried out using the adjusted NTP (2018) data for the combined tumor sites in mice and rats presented in Tables 6 and 7. These data sets demonstrated statistically significant increases in tumor incidence identified either by testing for a dose-response trend, or by a pairwise comparison of exposed animals with controls (or both).

Lifetime Average Daily Doses

The lifetime average daily dose (LADD) in units of mg/kg-day of PCBTF was calculated for each of the exposed groups, based on the exposure concentration, the average animal body weight (BW) and inhalation rate (IR), the daily exposure time, and the study duration. The average body weight for mice and rats was calculated from the data reported by NTP for control animals. The female and male mice weighed an average of 0.0442 kg and 0.0455 kg, respectively. The values for female and male rats were respectively 0.3096 kg and 0.5163 kg.

Table 6. Adjusted tumor incidence in mice exposed to PCBTF by inhalation (NTP, 2018) [a,b]								
Tumor type		**Incidence by concentration**				**Statistical p-values for pairwise comparison with controls** (p-value for trend in control column)			
	ppm	**0**	**100**	**200**	**400**	**0**	**100**	**200**	**400**
	mg/m^3	**0**	**740**	**1500**	**3000**	**0**	**740**	**1500**	**3000**
(Female mouse)									
Liver: Hepatocellular Adenoma, Hepatocellular Carcinoma, or Hepatoblastoma		18/47**	18/48	29/46*	46/47**	< 0.0001	0.614	0.014	< 0.0001
Harderian Gland: Adenoma or Adenocarcinoma		2/49*	6/49	9/49*	8/48*	0.036	0.134	0.025	0.042
(Male mouse)									
Liver: Hepatocellular Adenoma, Hepatocellular Carcinoma, or Hepatoblastoma		31/50**	37/50	40/49*	48/49**	< 0.0001	0.142	0.025	< 0.0001

(a) Incidence ratio after adjusting for intercurrent mortality using the effective number adjustment method.

(b) *p*-values are from pairwise comparisons with controls using Fisher exact tests performed by OEHHA; p-values in the control column are for Cochran-Armitage trend tests performed by OEHHA; * = *p*<0.05, ** = *p*<0.01.

Table 7. Adjusted tumor incidence in rats exposed to PCBTF by inhalation (NTP, 2018)								
Tumor type	**Incidence by concentration [a]**				**Statistical p-values for pairwise comparison with controls [b]** (p-value for trend in control column)			
ppm	0	100	300	1000	0	100	300	1000
mg/m^3	0	738	2214	7380	0	738	2214	7380
(Female rat)								
Adrenal Medulla: Benign or Malignant Pheochromocytoma	0.0%	10.7%	9.9%	13.5%*	0.106	0.071	0.085	0.035
Thyroid Gland (C-cell): Adenoma or Carcinoma	5.5%**	25.5%*	20.2%	33.6%**	0.009	0.017	0.057	0.002
Uterus: Stromal Polyp or Stromal Sarcoma	19.6%	23.8%	41.8%*	27.2%	0.439	0.440	0.028	0.298
Uterus: Adenocarcinoma	2.9%*	2.7%	0.0%	11.3%	0.017	0.748N [c]	0.475N	0.166
(Male rat)								
Lung: Alveolar/bronchiolar adenoma or Carcinoma	0.0%	5.3%	0.0%	9.3%	0.073	0.228	--	0.086
Thyroid Gland (C-cell): Adenoma or Carcinoma	7.6%**	13.4%	10.6%	39.2%**	< 0.001	0.326	0.481	< 0.001

(a) Rate percent after adjusting the number of animals at risk using the poly-3 adjustment method. Values are as reported by NTP (2018).

(b) Poly-3 p-values for pairwise comparison to the control group. The poly-3 trend p-value is provided in the control group column. Values are as reported by NTP (2018); * = p<0.05, ** = p<0.01.

(c) N = Decreased incidence.

The inhalation rate for mice, in m³/day, was calculated using the equation of Anderson *et al.* (1983) which was derived from experimental data:

$$IR_{mouse} = 0.0345 \times \left(\frac{BW_{mouse}}{0.025}\right)^{2/3}$$

In this equation, the constant 0.0345 is in m³/day, and the constant 0.025 and BW are in kg. The inhalation rate for rats was estimated using the following formula OEHHA (2018), with units corresponding to those in the above mouse equation:

$$IR_{rat} = 0.702 \times (BW_{rat})^{2/3}$$

The inhalation rates in m³/day were for mice: 0.0504 (female) and 0.0514 (male); and for rats: 0.3213 (female) and 0.4518 (male). LADDs were estimated using the following equation:

$$LADD = C_{air} \times \frac{IR}{BW} \times \frac{6.2}{24} \times \frac{5}{7}$$

where C_{air} is the exposure concentration of PCBTF in units of mg/m³, the factor 6.2/24 adjusts for six hours and 12 minutes per day exposure, and the factor 5/7 accounts for a five day-per-week dosing schedule. The LADDs of PCBTF administered in the studies are presented in Table 8.

Table 8: Lifetime average daily doses (LADDs) of PCBTF used in dose-response model			
Study animal	**Exposure concentration**		**LADD (mg/kg-day)**
	(ppm)	**(mg/m³)**	
Female mouse	0	0	0
	100	740	155
	200	1500	311
	400	3000	621
Male mouse	0	0	0
	100	740	154
	200	1500	308
	400	3000	615
Female rat	0	0	0
	100	740	141
	300	2200	424
	1000	7400	1413
Male rat	0	0	0
	100	740	119
	300	2200	356
	1000	7400	1192

Dose-Response Model

The mechanisms by which PCBTF induces tumors are not known. Given the limited available information pertaining to PCBTF's carcinogenic mode of action, OEHHA chose to model the tumor incidence data with its standard method, which uses the multistage cancer model and assumes that the dose-response relationship approaches linearity at low doses (OEHHA, 2009). According to the model, the life-time probability or risk of developing one or more tumors in a specific tissue as a function of dose is given as:

$$P(d) = 1 - \exp\left(-\beta_0 - \beta_1 d - \beta_2 d^2 \ldots - \beta_k d^k\right)$$

In the above equation, (d) represents the dose resulting from a uniform, continuous exposure over the nominal lifetime of the animal (two years for both mice and rats). The β_k are non-negative parameters, estimated by fitting the model to the

experimental data. When the dose is zero, the equation expresses the background tumor risk:

$$P_0 = 1 - \exp(-\beta_0)$$

OEHHA's cancer slope factors (CSFs) are estimates of the "extra risk" due to exposure. Extra risk is defined as the increased probability of tumor formation in an exposed population, divided by the probability of remaining tumor-free in the absence of exposure (i.e., the expected number of additional cases in an exposed group, divided by the expected number of tumor-free individuals in an unexposed population). This can be expressed as:

$$A(d) = \frac{P(d) - P_0}{1 - P_0}$$

where A(d) is the extra risk. Consequently, the multistage model for extra risk, as a function of dose, may be written as:

$$A(d) = 1 - \exp\left(-\beta_1 d - \beta_2 d^2 \ldots - \beta_k d^k\right)$$

For studies where the exposures vary in time, they are averaged over the entire study period and modeled as if they were uniform and continuous.

Model Calculations

OEHHA employed BMDS Version 2.7.0.4 (US EPA, 2017) to carry out the dose-response calculations for PCBTF. (The current version of BMDS is 3.1.1. In BMDS versions prior to 3.0, the multistage polynomial model for estimating cancer risk was referred to as the "multistage cancer" model in which the parameter estimates were restricted to be positive. In order to use the equivalent model in BMDS version 3.1.1, users must select the 'Frequentist Restricted" option on the multistage model.)

BMDS calculates a benchmark dose (BMD) based upon the maximum likelihood fit of the multistage model to the dose-response data and a chosen benchmark response (BMR). The 95% lower confidence level (BMDL) for the BMD is then estimated using the profile likelihood method. OEHHA fit the mouse and rat data to the multistage cancer equation using a benchmark response (BMR) of 5 percent. A graphical example of the multistage cancer model fitted to the male mouse liver tumor data is provided in Figure 2.

Figure 2: BMDS dose-response graph for male mouse liver tumors
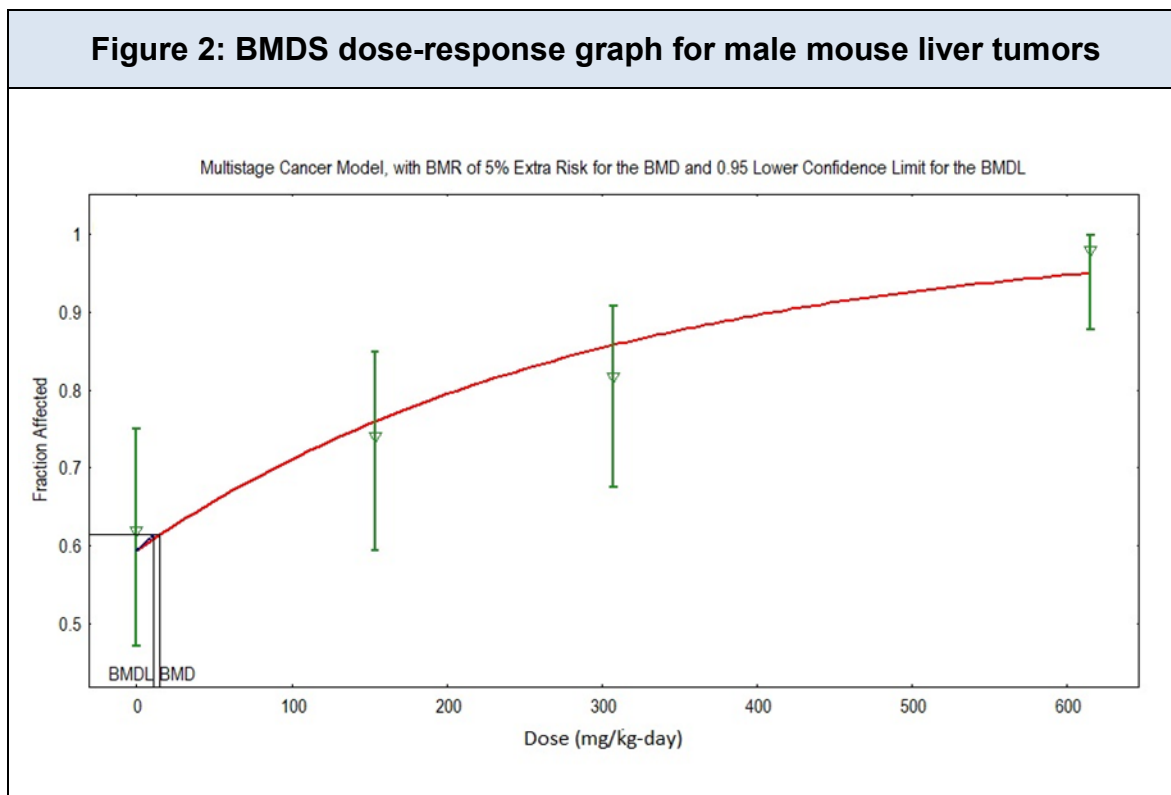
The model was run for each tumor site using polynomials of order one and two and the most appropriate model was chosen based on BMDS guidance developed by the US EPA (2014). Briefly, a goodness-of-fit p-value > 0.05, along with a small scaled-residual near the benchmark dose (absolute value < 2.0) indicates that the model fits the data well, and in cases where at least one model provides an adequate fit, the model with the lowest Akaike Information Criterion (AIC) value is often selected as the best fitting model. In cases where one or more of the model parameters (β_k) takes a value of zero upon fitting, and where more than one model provides an adequate fit to the data, the model with the lowest BMDL is chosen regardless of the AIC value.

Models using 1st degree polynomials were employed for all non-multisite cancer potency determinations, with the exception of female mouse hepatocellular adenomas, carcinomas, or hepatoblastomas, where a model using a 2nd degree polynomial was employed. For male and female mouse hepatocellular adenoma, carcinoma, or hepatoblastoma modeling, the model (1st or 2nd degree polynomial) with the lowest AIC was chosen.

For female mouse Harderian gland adenoma or adenocarcinoma modeling, the 1st degree polynomial model gave the same result as the 2nd degree model. This also occurred for the female rat adrenal medulla benign or malignant pheochromocytoma,

thyroid gland (C-cell) adenoma or carcinoma and uterine stromal polyp or sarcoma modeling.

Modeling of the following tumor types generated models where one or more of the model parameters (β_k) took a value of zero upon fitting, and more than one model provided an adequate fit to the data: female mouse Harderian gland adenomas or adenocarcinomas, male rat lung alveolar/bronchiolar adenomas or carcinomas and thyroid gland (C-cell) adenomas or carcinomas, and female rat uterine adenocarcinomas. In these cases, the more health-protective model was chosen regardless of the AIC, as recommended by US EPA (2014).

For combined uterine stromal polyps and sarcomas in female rats, the *p*-value for model fit was marginally acceptable at 0.07 and the ratio of the BMD to the BMDL was greater than five, indicating an increased level of uncertainty in the BMDL value. In this case, the tumor incidence observed in the highest dose group was inconsistent with the dose-response trend seen at the lower doses (See Table 6). In order to obtain a more acceptable fit to the model, OEHHA modeled this tumor by dropping the data from the highest dose group.

For carcinogens that induce tumors at multiple sites or in different cell types at the same site in a particular species and sex, OEHHA guidelines (2009) recommend the estimation of the multisite cancer risk. The multisite risk was estimated for male and female rats and for female mice since PCBTF induced tumors at multiple sites in these animals. The BMDS module for summing risks over several tumor sites uses a profile likelihood method, where the multistage model parameters (β_k) for each site are summed (e.g., $\Sigma\beta_0$, $\Sigma\beta_1$, $\Sigma\beta_2$) and the resulting model is used to determine a combined BMD. A confidence interval for the combined BMD is then calculated by computing the desired percentile of the chi-squared distribution associated with a likelihood ratio test having one degree of freedom. The single- and multisite BMDLs, along with several indicators of model performance, are presented in Table 9.

Table 9: BMDS Modeling Results								
Sex	**Tumor Types**	**Poly-nomial Degree**	**p-value for model fit**	**Scaled residual for dose near BMD**	**Model selection criterion** [(a)]	**BMD (mg/kg-day)**	**BMDL (mg/kg-day)**	**Animal CSF (mg/kg-day)**$^{-1}$
Mice								
M	Liver: hepatocellular adenoma, carcinoma, or hepatoblastoma	1	0.3998	0.371	Δ-AIC = 0.285	15.0416	10.521	4.752E-03
F	Liver: hepatocellular adenoma, carcinoma, or hepatoblastoma	2	0.3528	-0.836	Δ-AIC = 12.8	84.3596	43.5518	1.148E-03
F	Harderian gland: adenoma or adenocarcinoma	1	0.3735	0.506	One solution	179.859	99.1864	5.041E-04
F	Combined female mouse tumor risk	2	--	--	--	66.8647	35.647	1.403E-03
Rats								
M	Lung: alveolar/bronchiolar adenoma or carcinoma	1	0.0597	0.287	Low BMDL	816.064	329.086	1.519E-04
M	Thyroid gland (C-cell): adenoma or carcinoma	1	0.4586	0.54	Low BMDL	167.617	102.717	4.868E-04
M	Combined male rat tumor risk	1	--	--	--	139.056	84.1865	5.939E-04
F	Adrenal medulla: benign or malignant pheochromocytoma	1	0.0773	0.554	One solution	497.97	236.292	2.116E-04
F	Thyroid gland (C-cell): adenoma or carcinoma	1	0.0926	1.672	One solution	246.633	136.892	3.653E-04
F	Uterus: stromal polyp or sarcoma [(b)]	1	0.6465	-0.376	One solution	68.4765	37.8631	1.321E-03
F	Uterus: adenocarcinoma	1	0.2488	0.659	Low BMDL	988.415	458.092	1.091E-04
F	Combined female rat tumor risk	1	--	--	--	46.1297	24.5632	2.036E-03

(a) The final model selection was done following US EPA (2014) guidelines. "Δ-AIC" is the difference in AIC value between the chosen model and the alternative model. "One solution" indicates that optimization of the 2-degree polynomial model gave the same result as the 1-degree model. "Low BMDL" indicates that the more health-protective model was chosen regardless of the Δ-AIC, per US EPA (2014).

(b) In this instance, the data from the highest dose group was dropped in order to obtain an acceptable fit.

The cancer slope factors (CSFs) for mice and rats were derived from the BMDLs by dividing the BMR of 0.05 by the BMDLs. The dose-response assessment indicates that B6C3F1/N mice were more sensitive to the tumorigenic effects of PCBTF than Hsd:Sprague Dawley SD rats, with the male mouse being the most sensitive overall. Male mice were 3.5 times more sensitive than female mice, whereas female rats were about 3.5 times more sensitive than male rats. Male mice were 2.4 times more sensitive to exposure than were female rats.

Human Cancer Potency

Interspecies extrapolation from experimental animals to humans was based on the ratio of body weights raised to three-quarters power (US EPA, 2005; Anderson *et al.*, 1983), which for CSFs defined in units of reciprocal mg/kg-day, may be expressed in terms of the body-weight ratio raised to one-quarter power, as follows:

$$CSF_{human} = CSF_{animal} \times \left(\frac{BW_{human}}{BW_{animal}}\right)^{1/4}$$

The above scaling adjustment is presumed to account for the toxicokinetic and toxicodynamic differences between species. A default human body weight of 70 kg and the average body weights for mice and rats (see page 17) were used in the scaling formula. The resulting human CSFs are summarized below in Table 10.

The CSF based upon male mouse liver tumors, 2.976×10^{-2} (mg/kg-day)$^{-1}$, is the most health-protective of the four values that were derived from the NTP (2018) study data. This value, rounded to 3.0×10^{-2}, was chosen per OEHHA guidelines (2009) as the most appropriate estimate of PCBTF's carcinogenic potency in humans. An inhalation unit risk (IUR) of 8.6×10^{-6} (µg/m^3)$^{-1}$ is obtained by multiplying the CSF by a standard breathing-rate factor of 20/70 (m^3 per kg BW) and converting from milligrams to micrograms (1 mg/1000 µg):

$$IUR = CSF \left(\frac{20}{70 \times 1000}\right)$$

VI.   CONCLUSION

In this document, OEHHA has reviewed the available information relating to the potential carcinogenicity of PCBTF to humans exposed by inhalation. This information primarily consisted of: (1) studies on the toxicokinetics of PCBTF in rats, (2) studies investigating the potential for the chemical's genotoxicity in bacterial and mammalian cell cultures, as well as *in vivo* in rodents, and (3) a lifetime cancer evaluation of PCBTF in B6C3F1/N mice and Hsd:Sprague Dawley SD rats carried out by NTP (2018).

Table 10: Cancer slope factors					
Species	Sex	Tumor Sites	Animal BMDL (mg/kg-day)	Animal CSF (mg/kg-day)$^{-1}$	Human CSF (mg/kg-day)$^{-1}$
Mouse	M	Liver	10.521	4.752E-03	3.0E-02
Mouse	F	Liver + Harderian gland	35.647	1.403E-03	8.8E-03
Rat	M	Thyroid + Lung	84.1865	5.939E-04	2.0E-03
Rat	F	Thyroid + Adrenal gland + Uterus	24.5632	2.036E-03	7.9E-03

Data from the NTP (2018) study were used to identify the statistically significant, tumorigenic responses found in the study animals at various exposure levels. Data sets for estimating the cancer dose-response functions were developed based upon the related types of neoplasms found at each tumor site.

Prior to modeling, the data was adjusted to correct for increased rates of intercurrent mortality, which occurred in the more highly exposed mice and rats. In addition, external exposure concentrations (ppm) were converted to lifetime average daily doses (mg/kg-d). The BMDS multistage cancer model was then used to carry out the necessary mathematical operations. Since tumors were found at multiple sites in male and female rats and in the female mice, the aggregate cancer risk was also calculated for these animals, using the BMDS multi-site tumor module.

Four estimates of the human cancer slope factor were then obtained by weight-scaling the animal slope factors using the three-quarter-power scaling law (Table 9). The potency value derived from the male mouse liver tumor data, 3.0×10^{-2} (mg/kg-day)$^{-1}$ (8.6×10^{-6} (μg/m^3)$^{-1}$), was chosen as the best estimate for the human slope factor, consistent with OEHHA's policy of developing cancer potency factors that are adequate to protect public health (OEHHA 2009). As a final note, when compared to the database of cancer IURs adopted by OEHHA for the Hot Spots program (approximately 137 values), PCBTF falls within the lower 13 percent of IURs, indicating that the chemical has a relatively low cancer potency.

REFERENCES

Anderson EL and the Carcinogen Assessment Group of the US EPA (1983). Quantitative approaches in use to assess cancer risk. Risk Analysis 3(4):277-295.

Benigni R, Bignami M, Conti L, Crebelli R, Dogliotti E, Falcone E, Carere A. (1982). *In vitro* mutational studies with trifluralin and trifluorotoluene derivatives. Ann Ist Super Sanita 18(1):123-126.

Bignami M, and Crebelli R. (1979). A simplified method for the induction of 8-azaguanine resistance in *Salmonella typhimurium*. Toxicol Lett 3:169-175.

Brix AE, Hardisty JF, McConnell EE (2010). Combining neoplasms for evaluation of rodent carcinogenesis studies. In: Cancer Risk Assessment, C-H Hsu and T Stedeford eds, John Wiley & Sons, Inc. 619-715.

Gart JJ, Krewski D, Lee PN, Tarone RE, Wahrendorf J. (1986). Statistical methods in cancer research. Volume III--The design and analysis of long-term animal experiments. IARC Sci Publ:1-219.

Haworth S, Lawlor T, Mortelmans K, Speck W, Zeiger E. (1983). *Salmonella* mutagenicity test results for 250 chemicals. Environ Mutagen Suppl 1:3-142.

HSDB (2018). Hazardous Substances Data Bank. 1-Chloro-4-(trifluoromethyl) benzene, Chemical/Physical Properties. National Library of Medicine, Bethesda, MD. Available at: http://toxnet.nlm.nih.gov.

Knaak JB, al-Bayati MA, Raabe OG. (1995). Development of partition coefficients, Vmax and Km values, and allometric relationships. Toxicol Lett 79:87-98.

Knaak JB, Smith LW, Fitzpatrick RD, Olson JR, Newton PE. (1998). *In vitro* hepatic metabolism of PCBTF: Development of Vmax and Km values and partition coefficients and their use in an inhalation PBPK model. Inhal Toxicol 10:65-85.

Lee EG, Lewis B, Burns DA, Kashon ML, Kim SW, Harper M. (2015). Assessing Exposures to 1-chloro-4-(trifluoromethyl) Benzene (PCBTF) in U.S. Workplaces. J Occup Environ Hyg 12:D123-130.

Litton Bionetics, Inc. (1978a). Mutagenicity Evaluation of Parachlorobenzotrifluoride (PCBTF) in the Ames Salmonella/Microsome Plate Test, Final Report, (1978), US Environmental Protection Agency. Document No. 40-7852007, Fiche No. OTS0508133

Litton Bionetics, Inc. (1978b). Mutagenicity Evaluation of Parachlorobenzotrifluoride in the Mouse Lymphoma Forward Mutation Assay, Final Report (1978), US Environmental Protection Agency. Document No. 40-7852009, Fiche No. OTS0508135

Litton Bionetics, Inc. (1979a). Mutagenicity Evaluation of Parachlorobenzotrifluoride in a *In vivo*/*In vitro* Urine Assay, Final Report, (1979), US Environmental Protection Agency. Document No. 40- 7952013, Fiche No. OTS0508139

Litton Bionetics (1979b). Mutagenicity Evaluation of Parachlorobenzotrifluoride (PCBTF) in the Sister Chromatid Exchange Assay in L5178Y Mouse Lymphoma Cells Final Report (1979), US Environmental Protection Agency. Document No. 40-7952010, Fiche No. OTS0508136

Litton Bionetics Inc. (1980). Evaluation of *p*-Chlorobenzotrifluoride in the *In Vitro* Transformation of BALB/3T3 Cells Assay, Final Report, (1980), US Environmental Protection Agency. Document No. 40-8052018, Fiche No. OTS0508144

Lilly Research Laboratories (1983a). Chromosome aberrations in Chinese Hamster Ovary cells, test article compound 38502. (1983), US Environmental Protection Agency. Document No. 40-8452058, Fiche No. OTS0507306

Lilly Research Laboratories (1983b) Evaluation of compound #38502 in the Balb/c-3T3 neoplastic transformation assay with an aroclor-induced rat liver microsomal (S9) metabolic activation system. (1983). US Environmental Protection Agency. Document No. 40-8452058, Fiche No. OTS0507306

Macri A, Ricciardi C, Stazi AV, Mantovani A, Vendramin-Macri C, Piccioni A, Badellino E, Bianchi MP, Pepe M, Ceccanti M. (1987). Subchronic oral toxicity of 4-chloro-α,α,α-trifluoro-toluene in Sprague-Dawley rats. Food Chem Toxicol 25:781-786.

Mazza G, Dacarro C, Bonferoni C, Bonferoni B. (1986). Studies on the mutagenic activity of benzotrifluoride and twelve derivatives in microbial short-term assays. Farmaco Prat 41:215-225.

Microbiological Associates (1983). Activity of compound 38502 (T2025) in the acute *in vivo* cytogenetics assay in male and female rats, final report. (1983), US Environmental Protection Agency. Document No. 40-8452058, Fiche No. OTS0507306

Newton PE, Bolte HF, Richter WR, Akinsanya MB, Knaak JB, Smith LW. (1998). Inhalation toxicity, neurotoxicity, and toxicokinetic studies of *p*-chlorobenzotrifluoride. Inhal Toxicol 10(1):33-48.

NTP (1992). Toxicity studies of *p*-chloro-α,α,α-trifluorotoluene (CAS No. 98-56-6) administered in corn oil and α-cyclodextrin to F344/N rats and B6C3F1 mice in 14-day comparative gavage studies. Toxicity Report Series. Technical Report No. 14. National Toxicology Program, Research Triangle Park, NC.

NTP (2009). Chemical Information Profile for 1-Chloro-4-(trifluoromethyl)-benzene [CAS No. 98-56-6]; Supporting Nomination for Toxicological Evaluation by the National Toxicology Program. National Toxicology Program, National Institute of Environmental Health Sciences, June 2009.

NTP (2018). NTP Technical Report: Toxicology and Carcinogenesis Studies of *p*-Chloro-a,a,a-trifluorotoluene (CASRN 98-56-6) in Sprague Dawley Rats (Hsd:Sprague Dawley SD) and B6C3F1/N Mice (Inhalation Studies), TR 594. Research Triangle Park, NC, June 2018.

NCBI (2019). The PubChem BioAssay Database. National Center for Biotechnology Information. Online at: https://www.ncbi.nlm.nih.gov/pcassay?cmd=search.

OEHHA (2009). Air Toxics Hot Spots Program Risk Assessment Guidelines. Technical Support Document for Cancer Potency Factors: Methodologies for derivation, listing of available values, and adjustments to allow for early life stage exposures. California Environmental Protection Agency Office of Environmental Health Hazard Assessment. Online at: http://oehha.ca.gov/air/crnr/technical-support-document-cancer-potency-factors-2009.

OEHHA (2018). Calculation of rat breathing rate based on bodyweight. Office of Environmental Health Hazard Assessment. California Environmental Protection Agency Office of Environmental Health Hazard Assessment. Online at: https://oehha.ca.gov/media/downloads/crnr/calcuratbreathingrate092818.pdf.

OEHHA (2019). Safe Drinking Water And Toxic Enforcement Act Of 1986, Chemicals Known To The State To Cause Cancer Or Reproductive Toxicity. California Environmental Protection Agency, Office of Environmental Health Hazard Assessment. Online at: https://oehha.ca.gov/proposition-65/proposition-65-list

Pelosi GD, Oberdoerster J, Olson JR, Knaak JB, Smith LW, Newton PE. (1998). Characterization of rat hepatic cytochrome p-450 activities following inhalation exposure to *p*-chlorobenzotrifluoride. Inhalation Toxicology 10:49-63.

Portier CJ and Bailer AJ (1989). Testing for increased carcinogenicity using a survival-adjusted quantal response test. Fundam Appl Toxicol 12:731-737.

Quistad GB, Mulholland KM. (1983). Metabolism of *p*-chlorobenzotrifluoride by rats. J Agric Food Chem 31:585-589.

Rietjens IMCM, den Besten C, Hanzlik RP, van Bladeren PJ. (1997). Cytochrome P450-Catalyzed Oxidation of Halobenzene Derivatives. Chemical Research in Toxicology 10:629-635.

Shah RU, Coggon MM, Gkatzelis GI, et al. (2020). Urban Oxidation Flow Reactor Measurements Reveal Significant Secondary Organic Aerosol Contributions from Volatile Emissions of Emerging Importance. Environ. Sci. Technol. 54, 2, 714-725.

US EPA (2005). US Environmental Protection Agency. Guidelines for carcinogen risk assessment. Risk Assessment Forum. Report number EPA/630/P-03/001F.

US EPA (2014). Choosing Appropriate Stage of a Multistage Model for Cancer Modeling (BMDS Technical Guidance). US Environmental Protection Agency. https://cfpub.epa.gov/ncea/bmds/recordisplay.cfm?deid=308382.

US EPA (2016). Chemical Data Reporting Database for 2016. US Environmental Protection Agency. https://www.epa.gov/chemical-data-reporting.

US EPA (2017). Benchmark Dose Software (BMDS) version 2.7.0.4. US Environmental Protection Agency, National Center for Environmental Assessment, Research Triangle Park, NC 27711.

Yurawecz MP. (1979). Gas-liquid chromatographic and mass spectrometric identification of chlorinated trifluorotoluene residues in Niagara River fish. J Assoc Off Anal Chem 62:36-40.

ATTACHMENT 1

Kaplan-Meier Survival Curves for Mice and Rats
Presented in the NTP (2018) Study